Minimum thickness of carbon coating for multipacting suppression

M. Angelucci [1] A. Novelli [1,2] L. Spallino [1] A. Liedl [1] R. Larciprete [3,1] and R. Cimino [1,4]

[1]*LNF-INFN, Via E. Fermi 53, 00044 Frascati (Rome), Italy*
[2]*University of Rome "La Sapienza," Piazzale Aldo Moro 5, 00185 Rome, Italy*
[3]*ISC-CNR, Via dei Taurini 19 00185 Rome, Italy*
[4]*CERN, CH-1211 Geneva 23, Switzerland*

We performed a combined secondary electron yield and x-ray photoelectron spectroscopy study on a prototypical system formed by increasing coverages of amorphous carbon (*a*-C) deposited on atomically clean Cu. A remarkably thin *a*-C layer, of about 6–8 nm, is surprisingly enough to lower below 1 the secondary emission yield of the whole system. This feature qualifies such low thickness coatings as a optimal multipacting suppressor that will not significantly affect impedance issues. The concomitant reduction of surface conductivity observed after antimultipacting coating is, in fact, a major drawback, reducing its applicability in many research fields. The consequences of this observation are discussed mainly for *a*-C coating applications to mitigate detrimental multipacting effects in radio-frequency devices and accelerators, but are expected to be of interest for other research fields and to hold for other conductive substrates and overlayers.

Multipacting (MP) [1,2] is a resonant electron discharge, plaguing an extremely vast range of devices, produced by the synchronization of emitted electrons with the radio-frequency (rf) field (or with a passing beam, in accelerators) and by the electron multiplication at the impact point with the surface. An extremely vast range of research fields, spanning from Hall effect thrusters [3,4], divertors in tokamaks [5], high-power microwave systems for satellite applications [6–8], radio-frequency cavities [9–11] and antennas [12–14], optics for extreme ultraviolet (EUV) lithography [15], to particle accelerators [2,16,17] base some of their essential functionalities on the control and mitigation of multipacting. In particle accelerators, multipacting is better known as the "e^- cloud effect" [2]. Much of the ongoing research and development in all those fields are actively focused on reducing, in various ways, the number of electrons produced by a surface when hit by other electrons. This quantity, called secondary electron yield (SEY), is defined as the ratio of the number of emitted electrons (also called secondary electrons) to the number of incident electrons (also called primary electrons) [18] and is often called δ. Any solution that will decrease SEY around unity or below will grant full control of any detrimental MP effects and will become an essential ingredient in the design of many devices. Different approaches have been proposed to this end, one being to treat the device surfaces by coating them with intrinsically low SEY materials [2–7,9–13,16,17,19–26]. In satellite rf structures, Alodine (chromate conversion coating) has been the reference antimultipactor coating for the

space industry for decades because it presents a relatively low SEY, a good electrical conductivity, and it is very stable in air. However, a recent European Union (EU) directive prohibits manufacturers to use compounds with Cr^{+6} and new surface mitigators are therefore badly needed. In the research and development of accelerators, the quest for MP mitigators, generally called electron-cloud (EC) mitigators, is indeed a very hot topic since EC effects—generated in accelerator vacuum chambers by photoemission, residual-gas ionization, and secondary emission—can significantly affect the operation and performance of hadron and lepton accelerators. EC can induce increases in vacuum pressure, emittance growth, beam instabilities, beam losses, beam lifetime reductions, or additional heat loads on a (cold) chamber wall [2,17], and needs to be effectively reduced.

Coatings used as MP mitigation remedies must necessarily be compliant with a number of other stringent specifications, proper to the device under design. A low surface resistivity is a quite general and concurrent property required for device walls. Both in accelerators [16,27] and in rf cavities and antennas [13,28], the system requires the highest conductivity in the surface layers within the skin depth (typically ranging between some tenths to a few μm) characteristic of the electromagnetic (e.m.) interaction. Unfortunately, MP mitigator coatings are usually poor conductors. One line of research is then to try thinning the MP mitigator coating well below the size of this skin depth. A very thin coating, even if badly conductive, will not add any significant contribution to impedance. It is therefore of utmost importance to define not only the best coatings, but also their minimum thickness in order to have an effective MP mitigator with minimum impact on surface conductivity.

In this Rapid Communication, we present the results of SEY and x-ray photoelectron spectroscopy (XPS) measurements of a prototypical system, where an atomically clean

---

polycrystalline Cu substrate was incrementally covered by carbon layers of increasing thickness deposited by electron beam physical vapor deposition (EB-PVD). The experiment has been performed at the Material Science INFN-LNF laboratory of Frascati (RM), with a dedicated experimental apparatus which is described elsewhere [2,24–26,29–31]. Briefly, the UHV system includes a μ-metal chamber (pressure $\leqslant 1 \times 10^{-10}$ mbar) with less than 5 mG residual magnetic field at the sample position, dedicated to XPS and SEY analysis and a second chamber for *in situ* sample preparation. XPS spectra have been acquired with an Omicron EAC125 electron analyzer. Nonmonochromatic Mg $K\alpha$ radiation ($h\nu = 1253.6$ eV) has been used to induce photoemission. SEY is measured as described in detail in Refs. [2,24–26,29,30]. SEY (δ) is, by definition, equal to $I_{\text{out}}/I_p = (I_p - I_s)/I_p$, where I_p is the current of the primary electron beam hitting the sample, I_{out} is the electron current emerging from the sample, and I_s is the sample current to ground, as measured by a precision amperometer. I_p (some tens of nA) was measured using a Faraday cup positively biased, whereas I_s was determined by biasing the sample at -75 V. SEY curves as a function of the primary energy E_p are characterized by a maximum value (δ_{max}) reached at a certain energy (E_{max}). As already discussed [30], we can correctly measure SEY starting from $E_p \leqslant 1$ eV above the sample work function.

The polycrystalline, flat 8×8 mm^2 Cu sample was atomically cleaned by cycles of Ar$^+$ sputtering at 1 kV and thermal annealing at temperatures between 800 and 1000 K. A cleaned Cu substrate, even if not representative for realistic devices, was chosen to minimize all other spurious effects, such as electron-beam-induced SEY modification [24]. Carbon was deposited by means of an electron beam evaporator (Tectra GmbH) from a 99.999% purity C rod at room temperature. This method, if impractical for industrial productions, allows a very careful monitoring of the thickness, especially at very low coverages, and produces a very stable growth rate of well controlled and clean amorphous carbon (*a*-C) films. The results can then be extrapolated to other materials. Carbon was chosen for its known low SEY [22,23,25,26] and its undoubted capacity to be inert and very stable. During C evaporation, the background pressure was $\leqslant 5 \times 10^{-10}$ mbar. C layers, assumed to be reasonably homogeneous, were deposited during increasing time lapses and, after each evaporation, XPS and SEY analyses were performed. As discussed in the following, the XPS analysis confirms that *a*-C grows with a stable rate and allows one to convert deposition time to carbon coverage in nm [32], as used in this Rapid Communication.

In Fig. 1 the XPS survey spectra are shown, together with the C 1*s* and Cu 2*p* zoomed regions, for selected time deposition steps. In all spectra, there is no evidence of contaminants (as oxygen, etc.), confirming, in the limit of XPS sensitivity (some %), the cleanliness of our sample trough the entire growth/measurement process. Since the first deposition, C 1*s* is centered at the same binding energy as in highly oriented pyrolytic graphite (HOPG). There, it consists of a single component at 284.3 eV with a full width at half maximum (FWHM) lower than 0.3 eV [24,33,34]. In our data, the FWHM is ~1 eV, which is the convolution between the limited energy resolution of our experimental setup with the intrinsic broadening due to disorder. From the C 1*s* line
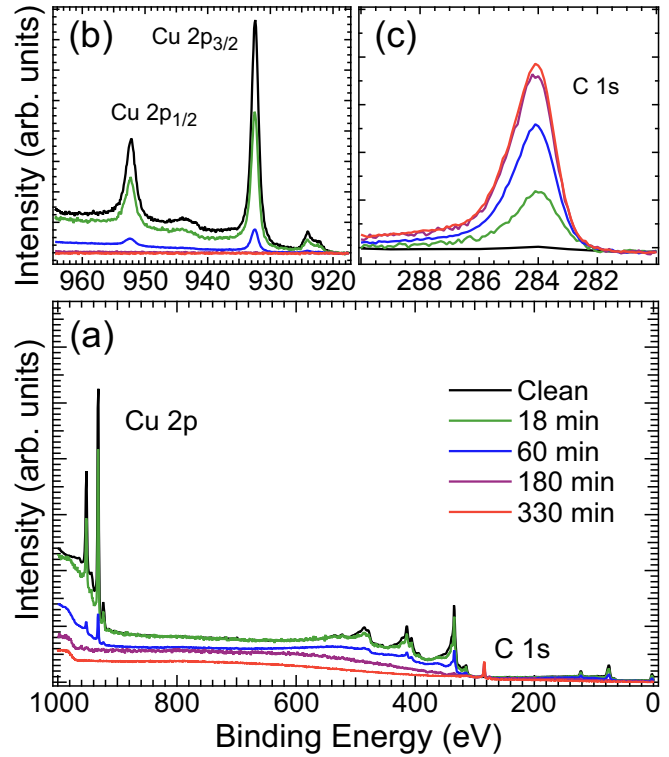

FIG. 1. (a) Survey, (b) Cu 2*p*, and (c) C 1*s* XPS spectra measured at different deposition times. In each XPS panel, the *Y* scales are kept constant to highlight the intensity variations.

shape and position, we conclude that, from early coverages on, carbon forms disordered sp^2 bonds. From the intensities of the characteristic peaks of each element, XPS allows one not only to perform an elemental composition analysis at the surface but also to quantify the *a*-C overlayer thickness [32,35–37].

As seen in Fig. 1, the Cu 2*p* core-level intensity decreases and C 1*s* increases upon *a*-C dosing as reported in Fig. 2. These trends are governed by the energy-dependent inelastic mean free path (IMFP) of the photoelectrons inside the overlayer. For the Cu 2*p* attenuation we can write the Beer-Lambert equation of the process as

$$I_{\text{Cu}} = I_{\text{Cu}}^{\text{clean}} e^{-d/\lambda_{\text{Cu-C}}} = I_{\text{Cu}}^{\text{clean}} e^{-t\,r/\lambda_{\text{Cu-C}}}, \tag{1}$$

where $I_{\text{Cu}}^{\text{clean}}$ is the clean substrate Cu 2*p* intensity; d is the unknown *a*-C thickness; and $\lambda_{\text{Cu-C}}$ is the IMFP of the Cu 2*p* photoelectron, generated in the copper substrate and traveling inside the carbon layers, with a kinetic energy of ≈ 310 eV. The coverage d is obtained by multiplying the evaporation time (t) and the evaporation rate (r), $d = t\,r$. Equation (1) can be used to fit the Cu 2*p* core-level intensity, as shown in Fig. 2, to find the deposition rate r, at a given $\lambda_{\text{Cu-C}}$, and therefore to evaluate the *a*-C coverage d. Analogously, the increase of the C 1*s* signal can be approximated by

$$I_{\text{C}} = I_{\text{C}}^{\text{max}}(1 - e^{-t\,r/\lambda_{\text{C-C}}}), \tag{2}$$

where $I_{\text{C}}^{\text{max}}$ is the saturated maximum value of the C 1*s* signal and $\lambda_{\text{C-C}}$ is the IMFP of the C 1*s* photoelectron, generated in the carbon layer and traveling inside it, with a kinetic energy of ≈ 970 eV. Given the sp^2 character of the *a*-C overlayer, we assume $\lambda_{\text{Cu-C}} \sim 0.9$ nm and $\lambda_{\text{C-C}} \sim 2.1$ nm
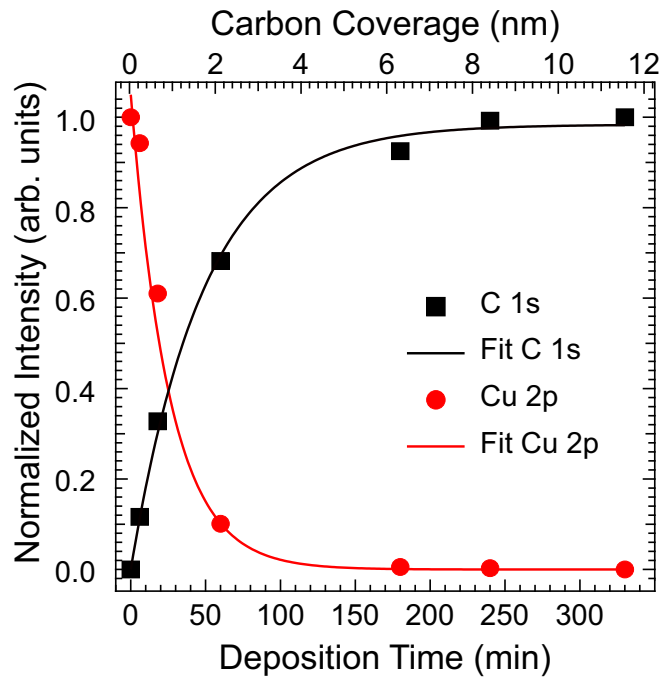
FIG. 2. Intensities of the C 1s and Cu 2p peaks at different deposition times and calculated a-C thicknesses. Beer-Lambert fits of the Cu 2p and C 1s intensity are also shown.

[35–39]. With those values, the resulting fits shown in Fig. 2 give a growth rate of 0.035 nm/min. Possible dishomogeneities in the growth morphology and variability in the IMFP for a-C suggest to give deposition coverages with an uncertainty of ±30%.
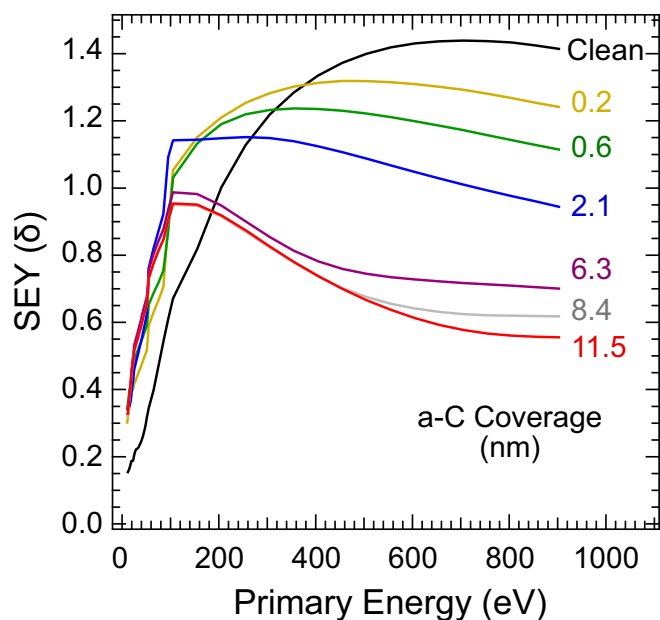

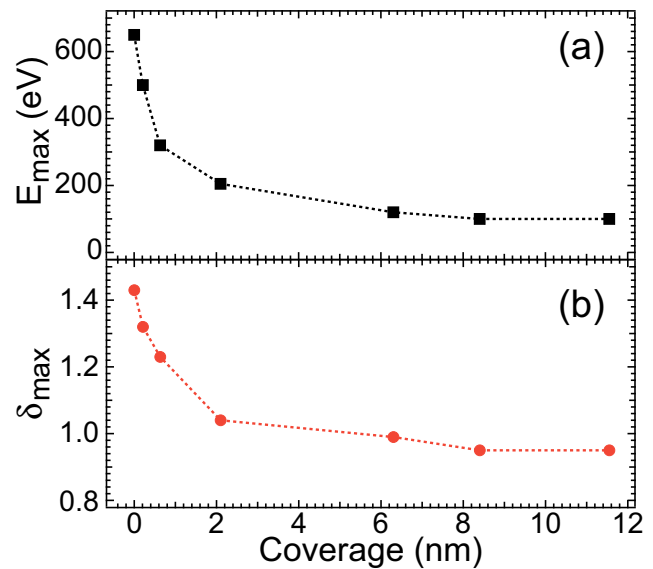FIG. 3. SEY (δ) measured as a function of carbon thickness (in nm).

FIG. 4. (a) E_{max} and (b) δ_{max} at different a-C thicknesses. $\Delta\delta_{max}/\delta_{max} = 5\%$ and $\Delta E_{max}/E_{max} = 10\%$.

It is therefore possible to follow the SEY evolution versus a-C coverage. This is shown in Fig. 3 and highlights a series of interesting issues:

(1) The SEY of the atomically clean polycrystalline Cu shows a δ_{max} of ∼1.4 at around $E_{max} \sim 640$ eV, consistent with literature results [2,30,40].

(2) For the initial low coverages of a-C, we notice some significant effect, especially in the very low-energy part of the SEY spectrum. This confirms how SEY, in this low-energy range, is sensitive to very small quantities of adsorbates and contaminants in the submonolayer regime [40].

(3) With increasing carbon coverages, the low-energy part of the SEY spectrum no longer changes significantly, while the overall curve is severely modified in shape, δ_{max} and E_{max}; δ_{max} is steadily reduced from ∼1.4 (clean copper) to less than 1 (after ∼6 nm of a-C) (see Fig. 4, bottom panel); also, E_{max} is significantly and steadily reduced with increasing a-C thickness, going from ∼650 eV (clean copper) to ∼100 eV after just ∼2 nm (see Fig. 4, top panel).

(4) For intermediate coverages, electrons emitted by the surface originate both within the substrate and the overlayer and the resulting SEY is governed by both material properties.

(5) After ∼6 nm, δ_{max} no longer changes, because it is dominated by the overlayer signal and SEY only marginally changes at high energies.

In Fig. 4 we report δ_{max} and E_{max} versus the estimated a-C coverage. On increasing the thickness, δ_{max} goes from the value of clean Cu to the one typically measured for graphite and a-C [25,26]. On the other hand, E_{max} starts from the clean Cu value but ends up significantly lower than what is observed in graphite and a-C. Something similar, if not so effective, was observed for E_{max} after repeated Ar$^+$ sputtering cycles on otherwise crystalline HOPG, implying that E_{max} could get reduced by increasing disorder (and/or amorphization) [26]. A detailed comparison, outside the scope of the present

Rapid Communication, between SEY of differently grown *a*-C films on Cu confirms the importance of morphology and local structure in determining the fine details of SEY.

The system studied here is prototypical and cannot be exploited for production both as due to the use of an atomically clean Cu substrate and for the EB-PVD to evaporate carbon.

We speculate that the minimum thickness identified here for *a*-C on Cu can be taken as valid for a large class of layer/substrate systems. The fact that after a coating of 6–8 nm, SEY is dominated by the overlayer properties, essentially depends on the intrinsic physical mechanisms governing the diffusion of electrons into solids [41]. The electron mean free path (MFP) can be reasonably approximated by a "universal curve," having a significant dependence on material conductivity only for low-energy electrons [35–39,42]. We expect that different metals and small gap semiconductor electronic properties will not significantly alter what we have observed at the *a*-C/Cu interface. The experimental method proposed here can be used anyway to confirm the generality of our results and/or studying in more detail special systems where, for instance, insulators are involved.

Our data call for a reexamination of the coating thickness normally used to mitigate MP. Even with safety margins (up to more than five times in thickness) typical of an industrial production, it is indeed possible to have a MP mitigator coating which only marginally affects the surface resistance within the skin depth and therefore is fully compliant with the impedance budget. Maybe the magnetosputtering deposition technique, routinely used for device coating on an industrial scale, is not easily controlled in this coverage regime and could either been implemented, modified, or even substituted with coating techniques more apt to control the quality of such thin films. What is clear here, in this context, is that 6–8 nm of *a*-C coating is enough to finally reduce SEY below 1. This observation would call for a technological effort to be able to reproduce and safely control, on an industrial scale, such low thickness coatings with the aim to finally produce MP mitigators that do not affect impedance.

In conclusion, we have studied a prototypical system formed by a thin *a*-C layer incrementally evaporated, at a low rate, on a polycrystalline Cu substrate. We address the question on what is the minimal layer thickness that defines the SEY of the system as the one of the overlayer and not of the substrate. We demonstrate that, in this case, 6–8 nm are sufficient to reduce the SEY from 1.4 (copper) to ∼1 (*a*-C). The results could be extrapolated to apply to other conductive bilayer systems and open up the possibility to design MP mitigators fully compliant with impedance issues.

[1] R. A. Kishek, Y. Y. Lau, L. K. Ang, A. Valfells, and R. M. Gilgenbach, Phys. Plasmas **5**, 2120 (1998).

[2] R. Cimino and T. Demma, Int. J. Mod. Phys. A **29**, 1430023 (2014).

[3] Y. Raitses, A. Smirnov, D. Staack, and N. J. Fisch, Phys. Plasmas **13**, 014502 (2006).

[4] I. Levchenko, S. Xu, G. Teel *et al.*, Nat. Commun. **9**, 879 (2018).

[5] J. P. Gunn, Plasma Phys. Controlled Fusion **54**, 085007 (2012).

[6] S. T. Lai, *Fundamentals of Spacecraft Charging: Spacecraft Interactions with Space Plasmas* (Princeton University Press, Princeton, NJ, 2011).

[7] A. Streltsov, J. Berthelier, A. Chernyshov *et al.*, Space. Sci. Rev. **214**, 118 (2018).

[8] C. Chang, G. Z. Liu, C. X. Tang, C. H. Chen, H. Shao, and W. H. Huang, Appl. Phys. Lett. **96**, 111502 (2010).

[9] R. F. Parodi, in *Proceedings of the CAS–CERN Accelerator School: RF for Accelerators, Ebeltoft, Denmark, 8–17 June 2010*, edited by R. Bailey, CERN-2011-007 (CERN, Geneva, 2011), p. 447.

[10] H. Padamsee, in *Proceedings of the CAS–CERN Accelerator School: Superconductivity for Accelerators, Erice, Italy, 24 April–4 May 2013*, edited by R. Bailey, CERN-2014-005 (CERN, Geneva, 2014), p. 141.

[11] I. Petrushina, V. N. Litvinenko, I. Pinayev, K. Smith, G. Narayan, and F. Severino, Phys. Rev. Accel. Beams **21**, 082001 (2018).

[12] G. Schoneman, V. Eveloy, M. Farrer *et al.*, in *The RF and Microwave Handbook*, edited by M. Golio (CRC Press, Boca Raton, FL, 2008).

[13] A. S. Gilmour, *Klystrons, Traveling Wave Tubes, Magnetrons, Crossed-Field Amplifiers, and Gyrotrons*, Artech House Microwave Library (Artech House, Boston, MA, 2011).

[14] R. A. Kishek and Y. Y. Lau, Phys. Rev. Lett. **80**, 193 (1998).

[15] J. Chen, E. Louis, J. Verhoeven, R. Harmsen, C. J. Lee, M. Lubomska, M. van Kampen, W. van Schaik, and F. Bijkerk, Appl. Surf. Sci. **257**, 354 (2010).

[16] A. W. Chao, K. H. Mess, M. Tigner, and F. Zimmermann, *Handbook of Accelerator Physics and Engineering*, 2nd ed. (World Scientific, Singapore, 2013).

[17] O. Malyshev, *Vacuum in Particle Accelerators: Modelling, Design and Operation of Beam Vacuum Systems* (Wiley, Hoboken, NJ, 2019).

[18] H. Seiler, J. Appl. Phys. **54**, R1 (1983).

[19] R. Valizadeh, O. B. Malyshev, S. Wang, S. A. Zolotovskaya, W. Allan Gillespie, and A. Abdolvand, Appl. Phys. Lett. **105**, 231605 (2014).

[20] R. Valizadeh, O. Malyshev, S. Wang, T. Sian, M. D. Cropper, and N. Sykes, Appl. Surf. Sci. **404**, 370 (2017).

[21] P. Chiggiato and P. Costa Pinto, Thin Solid Films **515**, 382 (2006).

[22] P. Costa Pinto, S. Calatroni, P. Chiggiato, H. Neupert, E. N. Shaposhnikova, M. Taborelli, W. Vollenberg, and C. Yin Vallgren, in *Proceedings, PAC 2011*, Vol. THOBS6 (CERN, Geneva, 2011).

[23] C. Yin Vallgren, G. Arduini, J. Bauche, S. Calatroni, P. Chiggiato, K. Cornelis, P. C. Pinto, B. Henrist, E. Métral, H. Neupert, G. Rumolo, E. Shaposhnikova, and M. Taborelli, Phys. Rev. ST Accel. Beams **14**, 071001 (2011).

[24] R. Cimino, M. Commisso, D. R. Grosso, T. Demma, V. Baglin, R. Flammini, and R. Larciprete, Phys. Rev. Lett. **109**, 064801 (2012).

[25] R. Larciprete, D. Grosso, A. Di Trolio, and R. Cimino, Appl. Surf. Sci. **328**, 356 (2015).

[26] L. A. Gonzalez, R. Larciprete, and R. Cimino, AIP Adv. **6**, 095117 (2016).

[27] M. Migliorati, E. Belli, and M. Zobov, Phys. Rev. Accel. Beams **21**, 041001 (2018).

[28] K. Lomakin, G. Gold, and K. Helmreich, IEEE Trans. Microwave Theory Tech. **66**, 2649 (2018).

[29] R. Cimino, I. R. Collins, M. A. Furman, M. Pivi, F. Ruggiero, G. Rumolo, and F. Zimmermann, Phys. Rev. Lett. **93**, 014801 (2004).

[30] R. Cimino, L. A. Gonzalez, R. Larciprete, A. Di Gaspare, G. Iadarola, and G. Rumolo, Phys. Rev. Spec. Top.–Accel. Beams **18**, 051002 (2015).

[31] L. Spallino, M. Angelucci, R. Larciprete, and R. Cimino, Appl. Phys. Lett. **114**, 153103 (2019).

[32] J. F. Watts and J. Wolstenholme, *An Introduction to Surface Analysis by XPS and AES* (Wiley, Hoboken, NJ, 2003).

[33] F. Sette, G. K. Wertheim, Y. Ma, G. Meigs, S. Modesti, and C. T. Chen, Phys. Rev. B **41**, 9766 (1990).

[34] R. Larciprete, D. R. Grosso, M. Commisso, R. Flammini, and R. Cimino, Phys. Rev. ST Accel. Beams **16**, 011002 (2013).

[35] C. J. Powell and A. Jablonski, J. Phys. Chem. Ref. Data **28**, 19 (1999).

[36] S. Tanuma, C. Powell, and D. Penn, Surf. Interface Anal. **43**, 689 (2011).

[37] G. Wilson and J. R. Dennison, IEEE Trans. Plasma Sci. **40**, 291 (2012).

[38] B. Ziaja, D. van der Spoel, A. Szöke, and J. Hajdu, Phys. Rev. B **64**, 214104 (2001).

[39] B. Lesiak, A. Jablonski, Z. Prussak, and P. Mrozek, Surf. Sci. **223**, 213 (1989).

[40] L. A. Gonzalez, M. Angelucci, R. Larciprete, and R. Cimino, AIP Adv. **7**, 115203 (2017).

[41] M. Dapor, *Transport of Energetic Electrons in Solids*, Springer Tracts in Modern Physics Vol. 999 (Springer, Cham, 2017).

[42] M. P. Seah and W. A. Dench, Surf. Interface Anal. **1**, 2 (1979).